CONFOCAL MICROSCOPY SEGMENTATION USING ACTIVE CONTOUR BASED ON ALPHA(α)-DIVERGENCE

L. Meziou[1], *A. Histace*[1], *F. Precioso*[2]

[1]ETIS UMR CNRS 8051,
[2]LIP6 UMR CNRS 7606,
[1]ENSEA, [1]UCP, [2]UPMC, France
firstname.lastname@ensea.fr

B. Matuszewski[3], *M. Murphy*[4]

[3]University of Central Lancashire, Preston, UK
[4]Liverpool John Moores University, UK
bmatuszewski1@uclan.ac.uk,
M.F.Murphy@ljmu.ac.uk

ABSTRACT

This paper describes a novel method for active contour segmentation based on foreground/background alpha-divergence histogram distance measure. In recent years a number of variational segmentation techniques have been proposed for a region based active contour segmentation utilising different distance measures between probability density functions (pdf) describing foreground and background regions. The most common techniques use χ^2, Hellinger/Bhattacharya distances or Kullback-Leibler divergence. In this paper, it is proposed to generalize these methods by using the alpha-divergences distance function. This distance function depending on the selected value of its parameter encompasses mentioned above classical distances. The paper defines a partial differential equation, associated with alpha-divergence variational criterion, that governs the iterative deformations of the active contour. The experimental results on a synthetic data demonstrate that the proposed method outperforms previously proposed histogram based methods in terms of segmentation accuracy and robustness with respect to type and level of noise. The potential of the proposed technique for segmentation of cellular structures in fluorescence confocal microscopy data is also illustrated.

Index Terms— Segmentation, active contour, alpha-divergence, confocal microscopy.

1. INTRODUCTION

A large variety of devices (MRI, TEP, X-RAY, CT-Scan, Cone-beam CT, laser or 3D confocal microscopy...) contemporarily used for acquisition of biomedical and medical data leads to the more and more challenging segmentation problems accounting for different characteristics of the acquired data including the diversity of associated acquisition noises (Gaussian, Poissonian, Rician, Speckle...). Among efficient segmentation methods in such context, active contour models have attracted extensive interest in the past two decades. Originally proposed in [1], the basic idea of the active contour is to iteratively evolve an initial curve towards the boundaries of target objects driven by a combination of internal forces, determined by the geometry of the evolving curve and the external forces induced from the image. The image segmentation method using active contour is usually based on minimizing a functional which is defined in such a way that it takes small values for curves close to the target boundaries. The functional minimization leads to a partial differential equation (PDE), constructed as the Gateaux derivative gradient flow which steers the evolution of the corresponding active contours.

In the particular framework of a region based active contours segmentation, some authors [2, 3, 4] have proposed to define a functional that takes into account the probability density functions (pdf) of both the inner and outer regions of the evolving curve. The variational criterion they proposed is based on the distances between pdfs related to the regions defined by the evolving curve and predefined reference pdfs of targeted object and background regions. Because of the characteristics of medical and biomedical images in which boundaries of target objects (organs, cells) are not well-defined and the fact that inner and outer intensity distribution can be quite similar (or at least the distribution overlap), such approaches can take into consideration complex prior information on the noise distributions of both object and background regions.

A first key issue for parametrization of these methods is the choice of the distance function (or similarity measure) between two pdfs. Common distances used to compare two pdfs are the χ^2 distance, the Kullback-Leibler divergence and the Hellinger/Bhattacharya distance [2, 3, 5]. In this article, we propose to introduce the alpha(α)-divergences as distance criterion between two pdfs. This choice is mainly motivated by the fact that this particular divergence family encompasses the aforementioned classical distances with respect to the value of α, and can thus provide more efficient distances than classical ones as we will show it in our experiments.

The work presented here focuses, first, on defining the PDE associated with alpha-divergence functional that will lead to the iterative deformations of the active contour and second, on the evaluation of this criterion on synthetic images (precision and robustness with respect to both level and type of noise) as compared to classical distances. Finally, in the context of the special session on "Analysis of Microscopy and Reconstructive Images for applications in Medicine and Biology", we present some preliminary results obtained on biomedical data. More precisely, these experiments illustrate the potential of the proposed segmentation methodology for automatic extraction of cellular structures (here we segment the nucleus) from actin tagged fluorescence confocal microscopy images.

2. HISTOGRAM BASED ACTIVE CONTOUR SEGMENTATION

2.1. Principle and governing PDE

The histogram based active contour methods are based on comparison between the normalized histogram (pdf) of the object to be seg-

The work presented in this paper has been in part supported from the TeRaFS project (EPSRC project No. EP/H024913/1).

mented (so-called foreground) and the normalized histogram of the background. Chan and Vese [6] worked with the assumption of a Gaussian intensity distribution for both object and background and pdfs having similar variances. This assumption is very restrictive since in typical images these distributions are multi-modal, especially for medical and biomedical data. The implementation of the histogram-based segmentation is described in [2, 3]. The method presented by Aubert *et al.* [2] compares the reference and estimated, from the data image, histograms for the background and foreground. Herbulot *et al.* [3] gives the general equation for active contour evolution with region-based criterion by considering normalized histograms of image features. In this framework, the formulation of the energy functional can be written:

$$\begin{aligned} J(\Gamma, \quad \Omega_{in} \quad , \Omega_{out}) &= \int_{\Re} \varphi(\hat{q}(\lambda, \Omega_{in}), \lambda) d\lambda \\ &+ \quad \int_{\Re} \varphi(\hat{q}(\lambda, \Omega_{out}), \lambda) d\lambda + \beta \int_{\Gamma} ds \end{aligned}$$

where Ω_{in} and Ω_{out} are respectively the foreground (targeted object) and the background of the image, Γ is the boundary between Ω_{in} and Ω_{out}, φ is a cost function related to a given measure of similarity between an estimated pdf $\hat{q}(\lambda, \Omega_i)$ ($i = in$ or out and $\lambda \in [0..2^n - 1]$, with the n intensity quantization levels) and a given reference pdf. Classically, $\hat{q}(\lambda, \Omega_i)$ are estimated using Parzen window approach as proposed in [3]. The reference pdfs are usually defined by a reference curve, segmented manually, that defines outer and inner pixels for each reference pdf. Subsequently, both reference pdfs are calculated using Parzen window method or parametrically if some priors on the pdf are known. The last term of Eq. (1) describes a regularization of the contour with β being a positive constant.

As proposed in [3], calculating the Euler derivative of Eq. (1), the corresponding evolution equation (PDE) of Γ is given by:

$$\begin{aligned} \frac{\partial \Gamma}{\partial t} &= [D(\Omega_{in}) - D(\Omega_{out}) + C(\Omega_{out}) - C(\Omega_{in}) \\ &+ \frac{1}{|\Omega_{in}|} \partial_1 \varphi_{in}(\hat{q}(\lambda), \lambda) * g_\sigma(\mathbf{I}(\mathbf{x})) \\ &- \frac{1}{|\Omega_{out}|} \partial_1 \varphi_{out}(\hat{q}(\lambda), \lambda) * g_\sigma(\mathbf{I}(\mathbf{x})) + \beta] \mathbf{N} \ , \end{aligned} \tag{1}$$

with

$$\begin{aligned} D(\Omega_i) &= \int_{\Omega_i} \varphi(\hat{q}(\lambda, \Omega_i), \lambda) d\lambda \\ C(\Omega_i) &= \int_{\Omega_i} \partial_1 \varphi(\hat{q}(\lambda, \Omega_i), \lambda) \hat{q}(\lambda, \Omega) d\lambda \\ i &= \{in, out\} \ . \end{aligned} \tag{2}$$

In Eqs. (1) and (2), $\partial_1 \varphi$ denotes the first order derivative of φ function with respect to $\hat{q}(\lambda, \Omega_i)$, g_σ represents the Gaussian kernel (with standard-deviation σ) used in estimation of $\hat{q}(\lambda, \Omega_i)$, $\mathbf{I}(\mathbf{x})$ the intensity function of the segmented image at a pixel $\mathbf{x}$, and $\mathbf{N}$ the inward local normal vector of the moving curve Γ.

Eq. (1) is composed of a global region term, involving $D(\Omega_i)$ and $C(\Omega_i)$, which are calculated on both foreground and background regions of the image, but also of a local term, calculated in a given neighborhood of Γ, that makes local refinement of the final segmented results.

For the classical φ functions proposed in the literature for measuring similarity between an estimated and a reference pdfs, the χ^2 function was originally proposed in [2], the Kullback-Leibler (KL) divergence and the Hellinger/Bhattacharya distance in [3]. In this article, we propose to introduce a different measure called the alpha-divergence that encompasses the aforementioned distances and provides thus more flexibility for the distance definition improving final segmentation results.

2.2. Alpha(α)-divergence as distance function

For any two pdfs $\hat{q}(\lambda, \Omega)$ (representing here the estimated pdf) and $q(\lambda)$ (representing the reference pdf), the alpha-divergence is defined as follows [7, 8]:

$$D_\alpha(\Omega) = \int_{\Omega} \varphi(\hat{q}(\lambda, \Omega), \lambda) d\lambda \ , \tag{3}$$

with

$$\begin{aligned} \varphi(\hat{q}(\lambda, \Omega), \lambda) &= \frac{1}{\alpha(1-\alpha)} \Big(\alpha \hat{q}(\lambda, \Omega) \\ &+ (1-\alpha) q(\lambda) \\ &- [\hat{q}(\lambda, \Omega)]^\alpha [q(\lambda)]^{1-\alpha} \Big) \ . \end{aligned} \tag{4}$$

where $\alpha \in]-\infty, +\infty[$.

Similarity measure of Eq. (4) verifies the following properties [9]:

1. $D_\alpha(\Omega)$ is convex with respect to both reference and estimated pdfs;
2. $D_\alpha(\Omega) \geq 0$;
3. $D_\alpha(\Omega) = 0$ when the probability distributions (here pdfs) are similar.

As a consequence, it can be considered as a distance between two pdfs. Moreover, considering Eq. (4), for specific values of α, classical distances can be connected to alpha-divergence, for instance :

- $D_2(\Omega) = \frac{1}{2} D_{\chi^2}(\Omega)$;
- $D_{\frac{1}{2}}(\Omega) = 2 D_{Hellinger}(\Omega)$;
- $D_{KL}(\Omega) = \frac{1}{2} \big(\lim_{\alpha \to 0} D_\alpha(\Omega) + \lim_{\alpha \to 1} D_\alpha(\Omega) \big)$.

This being said, it is possible to derive from Eq. (4) the first order derivative $\partial_1 \varphi$ associated to alpha-divergence similarity measure:

$$\partial_1 \varphi(\hat{q}(\lambda, \Omega), \lambda) = \frac{1}{\alpha - 1} \big(1 - [q(\lambda)]^{1-\alpha} [\hat{q}(\lambda, \Omega)]^{\alpha - 1} \big) \ , \tag{5}$$

which completely defines the evolution PDE of Eq. (1).

3. STATISTICAL EVALUATION OF THE PERFORMANCES ON SYNTHETIC IMAGES

In order to evaluate the performance of our criterion based on alpha-divergence, we have created a peanut shaped binary image subsequently generating different corrupted versions of this image (see Fig. 1) with a zero-mean Gaussian noise (which is the most common acquisition noise encountered), a Poisson noise (which characterizes scintigraphic imaging process or confocal microscopy), and a Rician noise (which is typical of MR imaging). Each of these noises has the same standard-deviation σ.

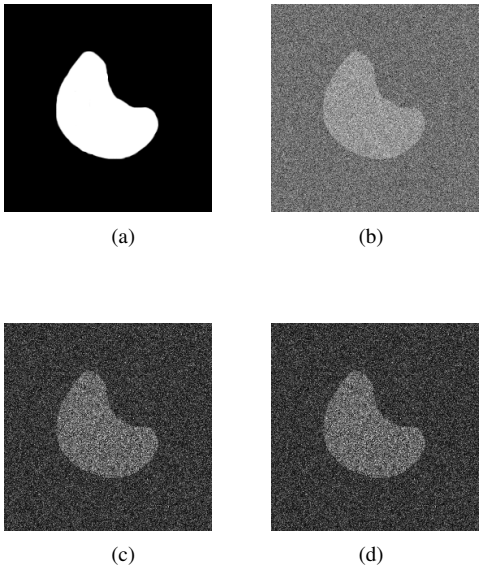

Fig. 1. Synthetic images used for segmentation tests: (a) Original binary image, (b) Gaussian noise, (c) Poisson noise and (d) Rayleigh noise. Here $\sigma = 150$.

To evaluate the performance of each distance criterion, we propose to evaluate the segmentation error (accuracy) through a quantization of the surface (expressed in pixels) defined by Γ curve at convergence compared to the original mask. Performances are evaluated for symmetric KL divergence, χ^2 and Hellinger distances (which corresponds to particular values of α), but also for intermediate values of α between 0 and 2. Results are aggregated in Tab. 1.

From a general point of view, these experiments allow a comparison between different similarity measures in the framework of histogram-based active contour segmentation. Some specific observations can be pointed out: Firstly, as it can be seen in Tab. 1, for each type of noise, there is at least one standard deviation σ where there is a value of α for which our method provide more accurate segmentation than any of previously proposed methods. For instance, the boundaries of a target object in an image corrupted by a Poisson noise with $\sigma = 150$ or 200 could be segmented more accurately by the "1.5-divergence" than by any other typically used distance criteria. Secondly, Tab. 1 tends to show a link between optimal α and the level of noise considered: For small noise levels ($\sigma = 100$ for instance), an alpha-divergence with a small α ($\alpha = 0.25$ or $\alpha = 0.5$) shows a better accuracy than any other tested method, and for a larger noise levels (σ up to 200), an alpha-divergence with a larger α ($\alpha = 1.5$ or 2) can provide better accuracy. These initial experiments show that the alpha-divergence criteria give access to a variability of distance measures that increases the adaptability of the histogram-based active contour segmentation approaches to image data exhibiting different pdfs distributions.

4. APPLICATION TO ACTIN TAGGED FLUORESCENCE CONFOCAL MICROSCOPY IMAGES

4.1. Framework

Actin is a principal component of the cytoskeleton playing an important role in cell biomechanics. Studies of its properties can be enhanced by providing information about its distribution within cell population. To address this, actin tagged fluorescence confocal microscopy is a promising imaging technique. However, a mandatory step to the characterization of the structural properties of actin is the segmentation of the nuclei and membranes of identified cells within acquired microscopic images. This task is very demanding due to highly complex cell appearances, a high level of noise (Poisson) and strong non-homogeneity of intensity and gradient information for such images (see Fig. 2). We propose here to show that histogram-based active contour segmentation using alpha-divergence is a promising technique for extraction of cell shapes from actin tagged fluorescence confocal microscopy. In the context of this paper, we first focus on the segmentation of nuclei of the cells.

4.2. Experiments

For the results shown in Fig. 2, all the tested segmentation methods were initialized with the same green contour which was also used for defining inner and outer regions for which reference pdf were computed. This green curve was manually drawn by an expert on a particular nucleus chosen for its central position within the image (see Fig. 2). *All nuclei are then segmented* using the inner pdf and the outer pdf of this green initial curve as reference pdfs and with a manual initialization of Γ drawn in order to embed the whole cell corresponding to the target nucleus. We can see on Fig. 2 that $\alpha = 1.5$ leads to a more accurate and satisfying segmentation than classical distances.

One could notice Fig. 2(b) that an "optimized" regularization version of Chan-Vese method can reach pretty good segmentation results. However, in order to obtain such results, some tests we made have shown that user has to specify both an initialization curve and a regularization parameter per nucleus to reach as satisfying results as those shown. This highly reduces the interest of Chan-Vese criterion in our experimental context.

Finally, Fig. 3, shows nuclei segmentation obtained on the adjacent slice to the one shown in Fig. 2 from the same 3D confocal microscopy acquisition. It is important to emphasize that these segmentations are obtained using the same pdf initialization and parameters as for the slice shown in Fig. 2. No new manual intervention of the expert was required. We illustrate hence the stability of our approach and its potential for fast automatic pre-segmentation of cell nuclei.

5. CONCLUSION

In this article, we have defined a new active contour criterion for biomedical image segmentation based on alpha-divergence of object and background pdfs. Our method outperfoms, in terms of segmentation accuracy and robustness, to both level and type of noises, all commonly considered distances to evaluate pdf similarity. The potential of our approach is illustrated on 3D confocal microscopy data. The next step is to automatically select a value of α parameter relying on the type and the level of noise in the data.

6. REFERENCES

[1] M. Kass, A Witkin, and D. Terzopoulos, "Snakes: Active contour models," *Int. J. Comput. Vision*, vol. V1, no. 4, pp. 321–331, January 1988.

[2] G. Aubert, M. Barlaud, O. Faugeras, and S. Jehan-Besson, "Image Segmentation Using Active Contours: Calculus Of Variations Or Shape Gradients?," *SIAM J. Applied Mathematics*, vol. 63, no. 6, pp. 2128–2154, 2003.

Noise Type	Gaussian			Rician			Poisson		
Noise Level : σ	100	150	200	100	150	200	100	150	200
$\alpha \to 0 \| 1$ (Kullback-Leibler)	0.56	0.85	1.28	0.52	1.11	2.19	0.5	0.64	1.26
$\alpha = 0.25$	0.6	0.73	1.07	**0.5**	0.93	2.13	**0.44**	0.74	0.85
$\alpha = 0.5$ (Hellinger)	**0.46**	0.77	1.19	0.6	**0.79**	1.58	0.55	0.58	0.76
$\alpha = 0.75$	0.57	**0.56**	1.08	0.56	0.72	2.04	0.64	0.53	1.17
$\alpha = 1.5$	0.86	0.68	1.08	1.15	0.99	1.54	0.69	**0.52**	**0.71**
$\alpha = 2$ (χ^2)	0.93	0.74	**0.88**	0.57	0.89	**1.41**	0.69	0.58	0.92

Table 1. Accuracy(%) estimations of the histogram based segmentation process for different values of α and for different kind and level of corrupting noise. In each case, the best result appears in bold letters.

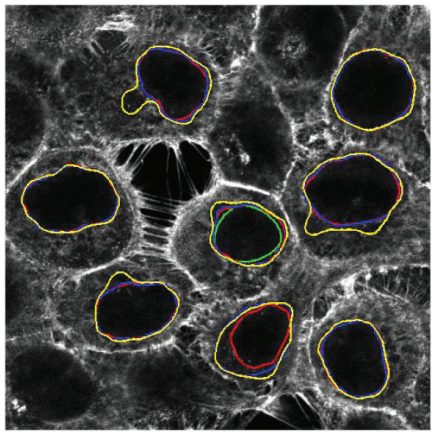

(a)

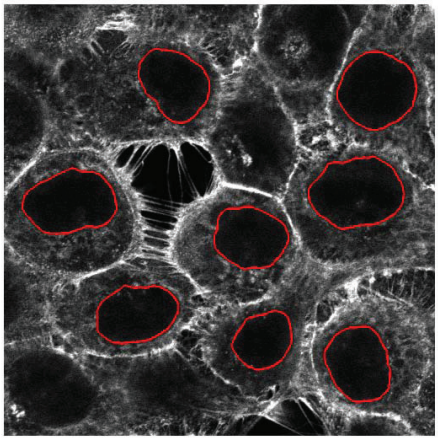

(b)

Fig. 2. (a) :Segmentation comparison for different values of α: $\alpha = 0$ (i.e. KL, red), $\alpha = 1.5$ (blue), $\alpha = 2$ (i.e. χ^2, yellow), in green, manual segmentation performs by a specialist for computation of inner and outer reference pdfs. (b) :Chan & Vese approach requiring for each nucleus a specific regularization settings.

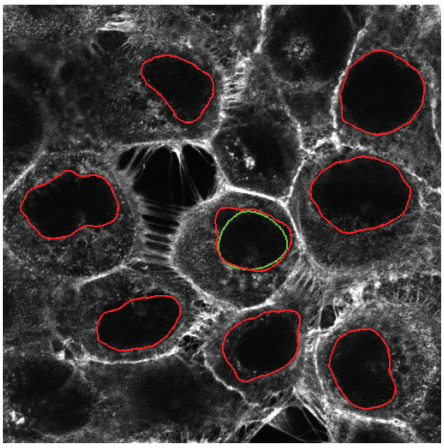

Fig. 3. Segmentation results for $\alpha = 1.5$ on a slice of 3D confocal microscopy acquisition next to Fig. 2 from previous slide pdf initialization (green curve is shown here as a reminder) with same parameters.

[3] A. Herbulot, S. Jehan-Besson, S. Duffner, M. Barlaud, and G. Aubert, "Segmentation of vectorial image features using shape gradients and information measures," *Journal of Mathematical Imaging and Vision*, vol. 25, no. 3, pp. 365–386, 2006.

[4] F. Lecellier, M.J. Fadili, S. Jehan-Besson, G. Aubert, M. Revenu, and E. Saloux, "Region-based active contours with exponential family observations," *Journal of Mathematical Imaging and Vision*, vol. 36, no. 1, pp. 28–45, January 2010.

[5] K. Ni, X. Bresson, T. Chan, and S. Esedoglu, "Local histogram based segmentation using the wasserstein distance," *Int. J. Comput. Vision*, vol. 84, pp. 97–111, August 2009.

[6] T. F. Chan and L. A. Vese, "Active contours without edges," *IEEE Transaction on Image Processing*, vol. 10, no. 2, pp. 266–277, 2001.

[7] A.O Hero, B. Ma, O. Michel, and J.D. Gorman, "Alpha-divergence for classification, indexing and retrieval (revised)," Tech. Rep. CSPL-328, The University of Michigan, June 2002.

[8] H. Zhu and R. Rohwer, "Information geometric measurements of generalisation (technical report ncrg/4350)," Tech. Rep., Aston University, 1995.

[9] A. Beirami, V. Cevher, B. Bower, and K. Tsianos, "Proofs of alpha divergence properties," Tech. Rep. STAT 631 / ELEC 639, Rice University, September 2008.